Macromolecules
ARTICLE

Macromolecules **2010**, *43*, 5233–5237 **5233**
DOI: 10.1021/ma100549w

Conducting Thiophene-Annulated Azepine Polymers

Changsik Song,[†,‡] D. Barney Walker,[†] and Timothy M. Swager*[,†,‡]

[†]*Department of Chemistry and* [‡]*Institute for Soldier Nanotechnologies, Massachusetts Institute of Technology, Cambridge, Massachusetts 02139*

Received March 10, 2010; Revised Manuscript Received May 12, 2010

ABSTRACT: We report the synthesis of annulated azepines, conjugated seven-membered ring systems with nitrogen, designed to undergo an electrochemically controlled bent-to-planar transformation driven by aromatization. A Pd-catalyzed double amination strategy enabled us to synthesize annulated azepines, which are thermally and electrochemically stable even in highly oxidized states. Several methods of chemical and electrochemical polymerization yielded azepine-based materials that were demonstrated to retain their redox properties in the solid state under ambient conditions. Because of their redox stability and conductivity, these polymers could find utility in actuating materials research.

Introduction

The development of electrochemically driven actuating polymers with a high degree of electrical to mechanical coupling is predicted to enable a range of micro- and nanomechanical devices, and several approaches are currently being pursued to achieve this goal.[1−10] Classically, the mechanical motion of electroactive materials is driven by either the Coulombic interaction between electrodes (in field activated actuators) or the reversible diffusion and intercalation of ions into the polymeric matrix following electrochemical oxidation (in ion diffusion activated actuators). Complementary to these approaches, several research groups[11−17] including our own[18−22] have become interested in developing materials in which a molecular-level geometrical change leads to macroscopic actuation.

In pursuit of designing such polymers, we have developed a number of systems containing moieties capable of extending and contracting in response to an electrochemical stimulus. Although our "molecular hinge" designs have predominantly been based on functionalized calixarenes, annulated heteropines (conjugated, heteroatom-bridged, seven-membered ring systems) also appear to be good candidates for molecular actuators as the energy gained from aromatization could be utilized to drive actuation. Being bent in their neutral state (8π electrons), heteropines can be planarized through oxidatively induced aromatization (6π electrons), leading to a significant dimensional change in the plane of the heteroannulene ring. We have recently demonstrated the design and synthesis of thiepin polymers;[23] however, these materials were shown to undergo desulfurization at high oxidation potentials. We have thus turned our attention to other heteroepine structures envisaged to have reversible redox properties. Herein we report on the design and synthesis of electrochemically and thermally stable azepine-based conjugated polymers.

Results and Discussion

Design and Molecular Modeling of Annulated Azepine Scaffold. We chose the nitrogen-containing azepine ring system to form the core of our annulated system for the following reasons. First, although related heteroepine systems with heavier atoms than sulfur (such as selenium[24−27]) can be accessed synthetically, they are expected to have low Se extrusion barriers[28] and would be likely to decompose on oxidation. Second, heteroepines containing heavier group 15 elements, such as phosphorus,[29] are easily oxidized to higher oxidation states (i.e., P^{5+}),[30,31] which would preclude the desired aromaticity-driven planarization. Lastly, the nitrogen-containing moiety can be incorporated at a late stage in the synthesis utilizing contemporary palladium-catalyzed amination reactions[32−35] enabling the modular preparation of prototype compounds.

To synthesize the target azepine core, we designed the periphery of the conjugated monomer units based on our previously reported thiepin system (Figure 1a, I−III). Both dithieno[2,3-*b*:3′,2′-*f*]azepines (type II) and isomeric dithieno-[3,2-*b*:2′,3′-*f*]azepines (type III) fit our design specifications. However, structures based on the type II design proved difficult to access in significant quantities (*vida infra*), and thus molecular modeling discussions are focused on variations of type III annulenes.

As expected, DFT calculations (B3LYP, 6-31G) suggested that type III azepines would adopt a bent geometry in the neutral state (Figure 1b and Supporting Information). However, it appeared that the degree of nonplanarity depended on the steric bulk of the N-substituents (R′). In the molecular models the distance between the outmost carbons (C3 and C10) decreased, indicating a more bowed annulene (when R′ = *p*-tolyl) compared with the unsubstituted analogue (where R′ = H), suggesting that steric crowding could augment the predisposition of the 8π electron azepine core to adopt a kinked conformation. However, the substituent effect was also found in the optimized geometries of the dicationic type III azepines. When R′ = H, the oxidized annulene appears to have a completely flat conformation, whereas when R′ is more sterically demanding (e.g., R′ = Me, *p*-tolyl), the geometry is distorted slightly from a planar conformation. Nevertheless, based on our calculations, oxidation of the annulated azepine should give rise to a structural expansion of around 5% and could potentially form the molecular basis for an actuating polymer.[36]

Synthesis of Thiophene-Annulated Azepines. We originally attempted to synthesize the type II azepines using a ring closing double amination strategy based on palladium-catalyzed C−N bond formation as pioneered by Buchwald and Hartwig.[32−35] Although a similar approach has been previously employed to assemble dithienopyrrole derivatives,[37]

*To whom correspondence should be addressed. E-mail: tswager@mit.edu.

Published on Web 05/21/2010

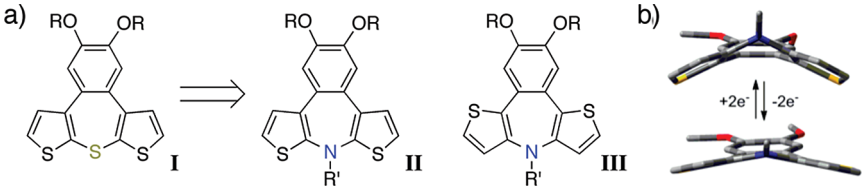

Figure 1. (a) Illustration of the design of annulated azepines (II and III) based on previously reported thiophene structure (I). The thiophene units were incorporated either side of the azepine ring to impart electrochemical stability and to allow for functionalization in the α-positions (C3 and C10). (b) DFT optimization (B3LYP, 6-31G) of an annulated azepine (R = R′ = Me) in its neutral (top) and oxidized (bottom) states.

Scheme 1. Synthesis of Annulated Azepine Monomers and Conjugated Polymers[a]

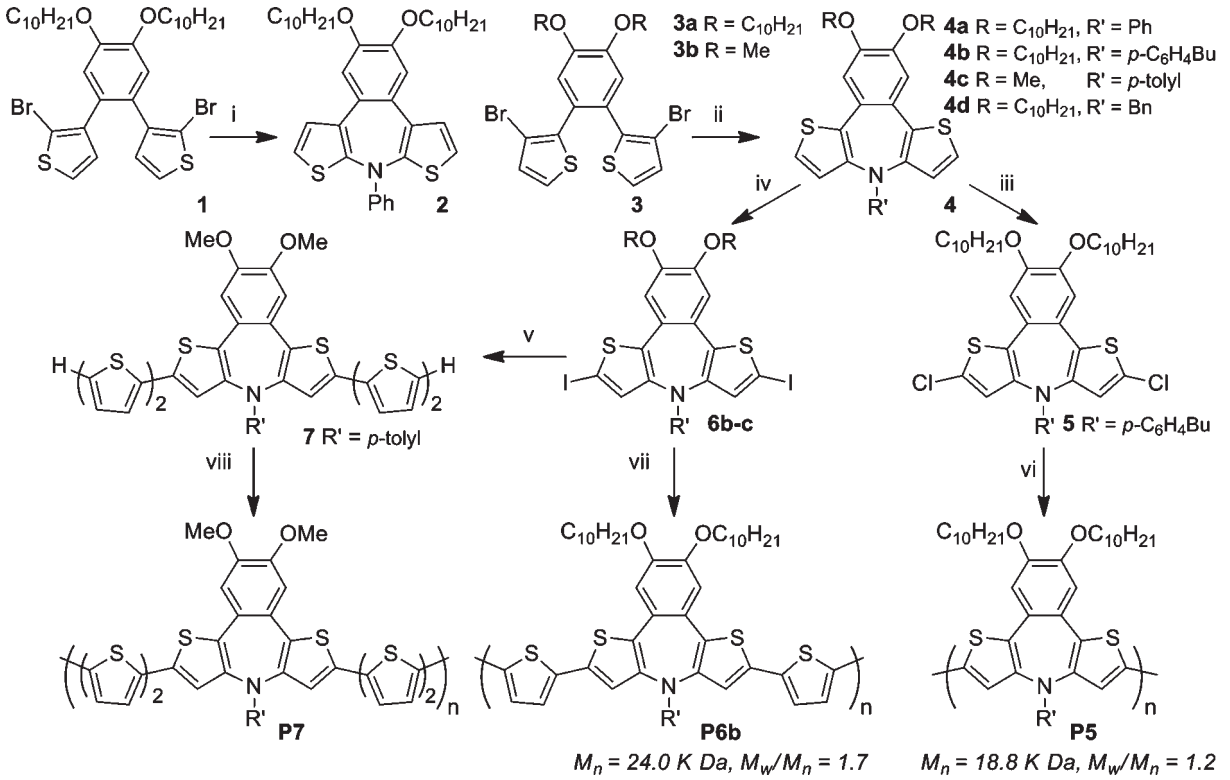

[a] Reagents: (i) $Pd_2(dba)_3 \cdot CHCl_3$, *t*-Bu_3PH-BF_4, NaO*t*-Bu, $PhNH_2$, PhMe, 100 °C, 24 h, 29%; (ii) $Pd_2(dba)_3 \cdot CHCl_3$, *t*-Bu_3PH-BF_4, NaO*t*-Bu, $ArNH_2$, PhMe, 100 °C, 24 h, 57−87% for **4a**−**c**, 24% for **4d**; (iii) *N*-chlorosuccinimide, $CHCl_3$, AcOH, room temperature, 16 h, 57%; (iv) *n*-BuLi, THF, −78 °C; then I_2, room temperature, 16 h, 58−91%; (v) $PdCl_2(PPh_3)_2$, 2-tributylstannylthiophene or 5-tributylstannyl-2,2′-bithiophene, DMF, 80 °C, 16 h, 55/85%; (vi) $Ni(cod)_2$, bipy, DMF/PhMe, 80 °C, 72 h, 66%; (vii) $Pd(PPh_3)_4$, 5,5′-bis(trimethylstannyl)-2,2′-bithiophene, PhMe, 80 °C, 72 h, 72%; (viii) $FeCl_3$, $CHCl_3$, room temperature, 15 h, 41%.

azepine-type compounds have not previously been prepared using this methodology. After optimization of reaction conditions we were eventually able to couple dibromide **1** with aniline to form azepine **2** in 29% yield with the remainder of the reaction mixture containing monoaminated product alongside multiple polar impurities resulting from substrate decomposition (Scheme 1, i).

This difficulty with the second ring-closing C−N bond formation is consistent with the findings of Hartwig and co-workers, who report (1) diarylamines react much more slowly when compared with *N*-methylaniline (the fastest) and aniline, (2) 3-bromothiophene reacts well with aniline but 2-bromothiophene does not, and (3) methyl substitution on the 3-position further reduces the reactivity of 2-bromothiophenes.[38] Furthermore, in a subsequent study[39] it is proposed that the amination of five-membered heteroaryl halides is dominated by the effectiveness of the reductive elimination step, which is unproductive in the case of the thiophen-2-yl-palladium amido complex. Thus, according to their findings, completion of the second amination is expected to be challenging. In our case the second amination is an intramolecular cyclization, which we suspect slightly mitigates some of the above undesirable effects.

In light of this we began to investigate the synthesis of type III dithieno[3,2-*b*:2′,3′-*f*]azepines. The double amination of dibromide **3a** to form azepine **4a** was significantly more effective using this approach, furnishing the desired azepine in 57% yield. Using this methodology, we were also able to access two other annulated *N*-arylazepines suitable for electrochemical investigation (**4b, 4c**) in 82% and 87% yield, respectively (Scheme 1, ii). In addition, we were able to synthesize benzyl analogue **4d** albeit only in 24% yield.[40]

Azepine monomer units suitable for polymerization were synthesized either by addition of *N*-chlorosuccinimide, to access **5**, or using a lithiation-iodine quenching sequence to obtain compounds **6b**−**c**. Of these, **6c** was characterized by X-ray crystallography (Figure 2). In the solid state the bent geometry of the neutral annulated azepine results in a distance of 6.41 Å between the outermost carbons, which is in good agreement with our DFT calculations (see Supporting Information).

Cyclic Voltammograms of Annulated Azepines. Cyclic voltammograms (CVs) of azepines **2**, **4a**, and **4d** were recorded in

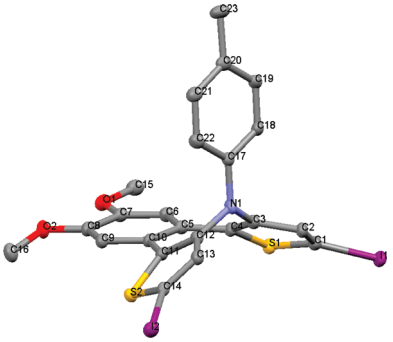

Figure 2. X-ray crystal structure of **6c**. The ellipsoid probability is 50%, and the hydrogens are omitted for clarity.

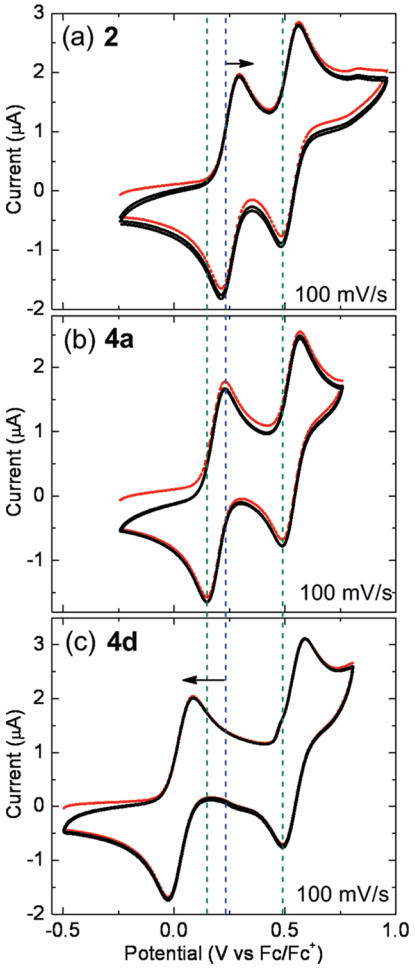

Figure 3. CVs of azepines **2** (a), **4a** (b), and **4d** (c) measured on Pt button electrodes in CH_2Cl_2 with 0.1 M $TBAPF_6$ as a supporting electrolyte. The red lines represent the first scans.

order to investigate the effect on redox properties of (a) the regiochemistry of the two thiophenes (type II vs type III azepines, **2** vs **4a**) and (b) the substituent on the azepine nitrogen (R′ = Ph vs R′ = Bn, **4a** vs **4d**). Using a standard three-electrode apparatus in CH_2Cl_2 with 0.1 M $TBAPF_6$ as a supporting electrolyte, reproducible CVs were obtained under ambient conditions (Figure 3). In all three cases the CVs showed two quasi-reversible one-electron redox waves. Interestingly, we observed significant differences in the potential at which the first ($E^1_{1/2}$ = 0.03−0.25 V vs Fc/Fc^+) but not the second oxidation ($E^2_{1/2}$ = ~0.53 V vs Fc/Fc^+). The half-wave potential for the first redox couple ($E^1_{1/2}$) of azepin **2** (0.25 V) was slightly

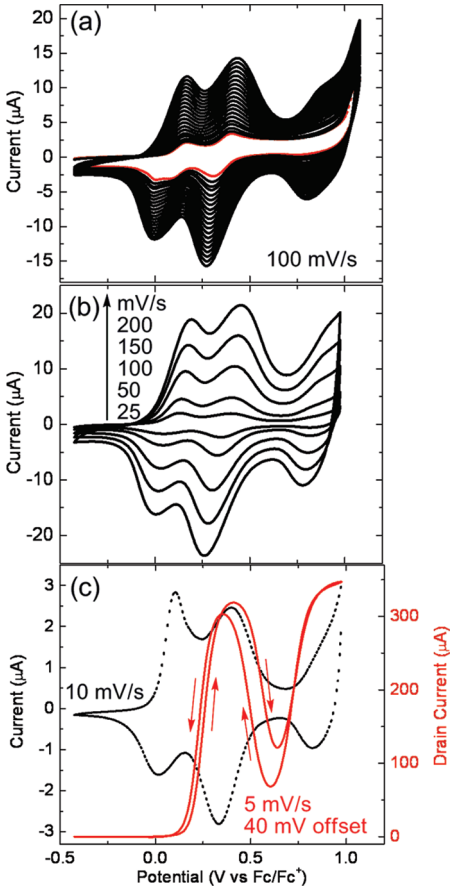

Figure 4. (a) Electropolymerization of **7** on a Pt button electrode in CH_2Cl_2 under ambient conditions. The red dotted lines represent the first scan. (b) CVs of films of **P7** at different scan rates. (c) CV (dotted lines) and *in situ* conductivity measurements (red solid lines) of films of **P7** on 5 μm interdigitated Pt microelectrodes in CH_2Cl_2. $TBAPF_6$ (0.1 M) was used as a supporting electrolyte in all measurements.

higher than that of azepine **4a** (0.19 V vs Fc/Fc^+). We suspect that the type II annulation stabilizes the oxidized compound more than type III annulations, a phenomenon we also observed in structurally related thiepin systems.[23] In the case of benzylazepine **4d**, the first oxidation $E^1_{1/2}$ has shifted to a lower potential (0.03 V vs Fc/Fc^+) compared with **4a**. We suspect that this difference is due to a slight inductive electron-donating effect of the benzyl group's CH_2 fragment.[41] Remarkably, all three of the second oxidations occur at almost the same potential, an observation that is not fully understood at this time.

Electropolymerization of Extended Azepines. Electropolymerizable azepine **7** was synthesized using a Stille cross-coupling reaction (Scheme 1, v), and a CH_2Cl_2 solution of the compound was exposed to swept potential conditions in the presence of 0.1 M $TBAPF_6$ as a supporting electrolyte. Despite the prediction of extended conjugated thiophenes to undergo electropolymerization, it was necessary to scan to relatively high oxidation potentials (~1.15 V vs Fc/Fc^+) in order to initiate polymer deposition on the platinum electrode (Figure 4a). We were not able to observe any film growth when we scanned at the low potential range (up to 0.98 V vs Fc/Fc^+, Supporting Information). For this particular system it is conceivable that initially developed radicals and charges are localized in the azepine moiety and are consequently not available for monomer−monomer coupling reactions. When a third oxidation peak was developed and the polymer started to be deposited, it became clear that **P7** has two distinct electroactive regions: the

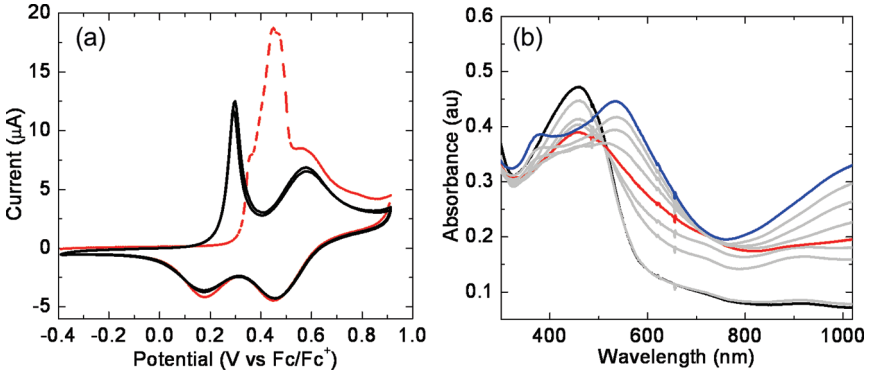

Figure 5. (a) CV of polymer **P6b** on a Pt button electrode (drop-cast from $CHCl_3$ solution) in CH_3CN with 0.1 M $TBAPF_6$ as a supporting electrolyte at a scan rate of 100 mV/s. The red dotted line represents the first potential sweep. (b) Electronic absorption spectra of polymer **P6b** on ITO-coated glass electrodes in CH_3CN with 0.1 M $TBAPF_6$ as a supporting electrolyte as a function of oxidation potential from 0.0 to 1.0 V vs Ag/Ag^+.

two-electron redox region localized in the azepine moiety and the pendant oligothiophene region. Subsequent analysis of scan rate dependence on the deposited polymer thin films in monomer-free CH_2Cl_2 electrolyte solution was demonstrated to be almost linear up to a scan rate of 200 mV/s, indicating that once **P7** is formed it has reversible redox properties (Figure 4b).

In situ conductivity measurements revealed several intriguing features of **P7** (Figure 4c). The drain current, which is proportional to conductivity, has its first maximum at the potential of the second oxidation. This bell-shaped conductivity profile is commonly observed in segmented (partially conjugated) polymers[18] and is indicative of a charge hopping phenomenon, which in this case is highest when there are equal number of singly and doubly oxidized azepine units. The latter part of the profile is a result of the oligothiophene segments. Hence, in the first oxidation, charges are strictly localized on the azepine moieties of **P7**. At the second oxidation, the oligothiophene portions start to be oxidized and the conductivity increases again. Given the doubly charged nature of azepine moieties, it is likely that at higher potentials the mobile carriers are localized to the thiophene segments and that conduction is dominated by interchain rather then intrachain transport. Repeated measurements did not diminish the electrochemical activity of **P7** under the experimental conditions, highlighting the stable nature of the azepine groups.

Chemical Synthesis, Redox Behavior, and Spectroelectrochemistry of Annulated Azepine Polymers. While electrochemical synthesis yielded material with promising electrical properties, the resultant polymer proved difficult to manipulate and characterize. Accordingly, we investigated various methods of chemical polymerization in order to generate material suitable ultimately for incorporation into devices. Using optimized Yamamoto homopolymerization conditions, dichloride **5** was converted into moderate molecular weight polymer **P5** (M_n = 18.8 kDa, PDI = 1.24) in 66% yield (Scheme 1, vi). We were also able to convert **6b** into conjugated polymer **P6b** (M_n = 24.0 kDa, PDI = 1.7) in 62% yield under Stille polymerization conditions using 5,5′-bis(trimethylstannyl)-2,2′-bithiophene as a comonomer (Scheme 1, vii). Following purification both polymers were drop-cast onto Pt electrodes and investigated using CV analysis in a 0.1 M CH_3CN solution of $TBAPF_6$. Under these conditions polymer **P5** displayed nonideal electroactivity and appeared to become largely inactive after the first potential cycle (see Supporting Information). Considering the high stability of the azepine unit, the loss of inactivity is likely due to a loss of electrical contact with the working electrode. This behavior may be a result of the larger strain imposed by having every segment undergoing a large redox-induced geometric change. In accord with this explanation, we observe two redox couples in the CV of polymer **P6b** (Figure 5a) similar to the electrochemical of parent compound **4a** (Figure 3b). The first oxidation peak for **P6b** was abnormally sharp, which implies that the CH_3CN did not swell the neutral polymer and thus initially impeded the diffusion of ions and accompanying solvent molecules. Once charged, the polymer is solvated by the CH_3CN, and ions diffused more readily into and out of the polymer. After the initial electrochemical oxidation/reduction cycle the CV adopted a more typical shape. Interestingly, during the first scan the onset potential was higher and the integrated current was larger when compared with successive scans. These changes are likely related to the reorganization of the polymer's microstructure caused by the geometric changes and solvent uptake/release during the initial potential cycle. The sharp character of the first oxidation wave after the break in of the film is consistent with the predicted geometric changes. Upon reaching the initial oxidation, the strain associated with a minority of azepine units adopting a planarized conformation prevents oxidation. This inhibition to oxidation results in increased current at higher potentials when the matrix relaxes.

To measure spectroelectrochemical properties, we drop-cast azepine polymer **P6b** onto an indium−tin oxide (ITO) coated glass electrode. Figure 5b illustrates the *in situ* measurements of UV−vis spectra following increased oxidation levels in CH_3CN: the black line represents the absorption at 0 V, the red line at 0.6 V, and the blue line at 1.0 V (all vs Ag/Ag^+). There are two regimes in the potential-dependent optical spectra that reveal the development of subgap absorptions. One is from 0 to 0.6 V and the other is from 0.6 to 1.0 V, and these roughly correlate with the first and second azepine oxidations, respectively. In the first regime, the original bandgap absorption decreased and new absorption increased in the subgap region. The new absorptions appear broad and featureless, implying that the polymer has a very delocalized electronic structure. However, the absorptions are more distinct in the second oxidation regime. It is an interesting feature that the original bandgap region retains a considerable amount of absorption while most polythiophene derivatives show considerable depletion of these absorptions on oxidation.[42]

We attempted to measure *in situ* conductivities from the azepine-incorporated polymer **P6b** by drop-casting the polymer on an interdigitated microelectrode. Unfortunately, we were not able to detect any drain current signals. This was most likely due to high contact resistance with the electrode as an absolute electrical conductivity of 1.5 S/cm was measured using a four-point probe and a drop-cast film of oxidized **P6b** (doping by saturation with iodine vapor).

In contrast, we were able to measure the *in situ* conductivity of chemically polymerized **P7**, which was prepared by

$FeCl_3$-mediated polymerization (Scheme 1, viii). Although **P7** showed poor solubility in common organic solvents and was thus intractable for conventional polymer characterization, a drop-cast slurry of the polymer in $CHCl_3$ onto an interdigitated microelectrode produced a functional device. In this case the CV and the *in situ* conductivity measured for chemically prepared **P7** (Supporting Information) have very similar features (the reversible two electron redox sweep and the bell-shaped conductivity curve) to the electrochemically prepared material (Figure 4c). It was not possible to measure the absolute electrical conductivity of the polymer using a four-point probe as the material was not readily formulated into a homogeneous film. We are currently pursuing free-standing films of azepine-incorporated polymers for electrochemical actuation testing.

Conclusion

In summary, we have designed and synthesized several structurally related annulated azepine moieties using the Pd-catalyzed Buchwald−Hartwig coupling to fuse the seven-membered ring in the key synthetic step. In contrast to previously reported thiepin systems, dithieno[3,2-*b*:2′,3′-*f*]azepines were found to be very stable even in highly oxidized states. Azepine polymers with a molecular weight between 18 and 24 kDa were accessed by both chemical and electrochemical means, and two of these materials were proved to display redox stable behavior analogous to their parent monomers in the solid state. Because of their high electrochemical stability, azepine-based polymers are promising candidates for molecular actuators and other related applications.

Acknowledgment. We thank Dr. Peter Müller for collecting and solving the X-ray crystal structure. C.S. and T.M.S. were supported by the U.S. Army through the Institute for Soldier Nanotechnologies under contract with the U.S. Army Research Office. We are grateful to the European Union for the Marie Curie International Outgoing Fellowship to D.B.W.

Supporting Information Available: Detailed experimental procedures for the synthesis of all compounds; crystallographic data for **6c**; geometry optimizations (DFT calculations) of annulated azepines; CVs of **P5** in CH_2Cl_2 and CH_3CN; CV and *in situ* conductivity measured for chemically prepared **P7**; ^1H and ^{13}C NMR's of all compounds. This material is available free of charge via the Internet at http://pubs.acs.org.

References and Notes

(1) Baughman, R. H. *Synth. Met.* **1996**, *78*, 339–353.
(2) Anquetil, P. A.; Yu, H. H.; Madden, J. D.; Madden, P. G.; Swager, T. M.; Hunter, I. W. *Proc. SPIE Int. Soc. Opt. Eng.* **2002**, *4695*, 424−434.
(3) Smela, E. *Adv. Mater.* **2003**, *15*, 481–494.
(4) Yu, H. H.; Swager, T. M. *IEEE J. Oceanic Eng.* **2004**, *29*, 692–695.
(5) Almutairi, A.; Yoon, K.; Tham, F.; Marsella, M. J. *Pure Appl. Chem.* **2006**, *78*, 777–781.
(6) Kay, E. R.; Leigh, D. A.; Zerbetto, F. *Angew. Chem., Int. Ed.* **2007**, *46*, 72–191.
(7) Mirfakhrai, T.; Madden, J. D. W.; Baughman, R. H. *Mater. Today* **2007**, *10*, 30–38.
(8) Bar-Cohen, Y.; Zhang, Q. M. *MRS Bull.* **2008**, *33*, 173–181.
(9) Huang, T. J. *MRS Bull.* **2008**, *33*, 226–231.
(10) Li, D. B.; Paxton, W. F.; Baughman, R. H.; Huang, T. J.; Stoddart, J. F.; Weiss, P. S. *MRS Bull.* **2009**, *34*, 671–681.
(11) Marsella, M. J.; Reid, R. J. *Macromolecules* **1999**, *32*, 5982–5984.
(12) Marsella, M. J.; Reid, R. J.; Estassi, S.; Wang, L. S. *J. Am. Chem. Soc.* **2002**, *124*, 12507–12510.
(13) Liu, Y.; Flood, A. H.; Bonvallett, P. A.; Vignon, S. A.; Northrop, B. H.; Tseng, H. R.; Jeppesen, J. O.; Huang, T. J.; Brough, B.; Baller, M.; Magonov, S.; Solares, S. D.; Goddard, W. A.; Ho, C. M.; Stoddart, J. F. *J. Am. Chem. Soc.* **2005**, *127*, 9745–9759.
(14) Schafmeister, C. E.; Brown, Z. Z.; Gupta, S. *Acc. Chem. Res.* **2008**, *41*, 1387–1398.
(15) Chebny, V. J.; Shukla, R.; Lindeman, S. V.; Rathore, R. *Org. Lett.* **2009**, *11*, 1939–1942.
(16) Clark, P. G.; Day, M. W.; Grubbs, R. H. *J. Am. Chem. Soc.* **2009**, *131*, 13631.
(17) Fang, L.; Hmadeh, M.; Wu, J. S.; Olson, M. A.; Spruell, J. M.; Trabolsi, A.; Yang, Y. W.; Elhabiri, M.; Albrecht-Gary, A. M.; Stoddart, J. F. *J. Am. Chem. Soc.* **2009**, *131*, 7126–7134.
(18) Yu, H. H.; Xu, B.; Swager, T. M. *J. Am. Chem. Soc.* **2003**, *125*, 1142–1143.
(19) Yang, Y.; Swager, T. M. *Macromolecules* **2006**, *39*, 2013–2015.
(20) Yang, Y.; Swager, T. M. *Macromolecules* **2007**, *40*, 7437–7440.
(21) Song, C.; Swager, T. M. *Org. Lett.* **2008**, *10*, 3575–3578.
(22) Takita, R.; Song, C.; Swager, T. M. *Org. Lett.* **2008**, *10*, 5003–5005.
(23) Song, C.; Swager, T. M. *J. Org. Chem.* **2010**, *75*, 999–1005.
(24) Schwan, A. L. *Sci. Synth.* **2004**, *17*, 717–748.
(25) Schwan, A. L. *Sci. Synth.* **2004**, *17*, 705–716.
(26) Shirani, H.; Janosik, T. *Organometallics* **2008**, *27*, 3960–3963.
(27) Shirani, H.; Bergman, J.; Janosik, T. *Tetrahedron* **2009**, *65*, 8350–8353.
(28) Murata, I.; Nakasuji, K. *Top. Curr. Chem.* **1981**, *97*, 33–70.
(29) Borst, M. L. G.; Bulo, R. E.; Winkel, C. W.; Gibney, D. J.; Ehlers, A. W.; Schakel, M.; Lutz, M.; Spek, A. L.; Lammertsma, K. *J. Am. Chem. Soc.* **2005**, *127*, 5800–5801.
(30) de Meijere, A., Diederich, F., Eds.; *Metal-Catalyzed Cross-Coupling Reactions*, 2nd completely revised and enlarged edition; Wiley-VCH: Weinheim, Germany, 2003; Vol. *1*.
(31) de Meijere, A.; Diederich, F., Eds.; *Metal-Catalyzed Cross-Coupling Reactions*, 2nd completely revised and enlarged edition; Wiley-VCH: Weinheim, Germany, 2003; Vol. *2*.
(32) Guram, A. S.; Rennels, R. A.; Buchwald, S. L. *Angew. Chem., Int. Ed.* **1995**, *34*, 1348–50.
(33) Louie, J.; Hartwig, J. F. *Tetrahedron Lett.* **1995**, *36*, 3609–3612.
(34) Hartwig, J. F. *Acc. Chem. Res.* **1998**, *31*, 852–860.
(35) Wolfe, J. P.; Wagaw, S.; Marcoux, J.-F.; Buchwald, S. L. *Acc. Chem. Res.* **1998**, *31*, 805–818.
(36) DFT calculations also suggest that the one-electron oxidation of azepines ($4n$ − 1 state) gives rise to a slight expansion toward a planar conformation, the degree of which is smaller than that of two -electron oxidation ($4n$ − 2 state). This conformational change is probably due to the delocalization of the charge generated, not the aromatic stabilization, and seems to be true for most $4n$-electron conjugated cyclic systems, including thiepins and [8]annulenes. Similar geometric rearrangements are found to occur as well in simple N-functionalized 3-aminothiophenes. See: Heth, C. L.; Tallman, D. E.; Rasmussen, S. C. *J. Phys. Chem. B* **2010**, *114*, 5275–5282.
(37) Martin, R.; Larsen, C. H.; Cuenca, A.; Buchwald, S. L. *Org. Lett.* **2007**, *9*, 3379–3382.
(38) Hooper, M. W.; Utsunomiya, M.; Hartwig, J. F. *J. Org. Chem.* **2003**, *68*, 2861–2873.
(39) Hooper, M. W.; Hartwig, J. F. *Organometallics* **2003**, *22*, 3394–3403.
(40) It is known that β-hydride elimination is a competing side reaction with alkylamines, and the process can lead to dehalogenated products. The undesired β-hydride elimination can be suppressed by the use of bidentate ligands, such as 2,2′-bis(diphenylphosphino)-1,1′-binaphthyl (BINAP) or 1,1′-bis(diphenylphosphino)ferrocene (dppf). In this case we were not able to obtain the desired product with monodentate ligand t-Bu_3P, and switching to the BINAP ligand furnished the desired *N*-benzylazepine **4d**. However, the yield was low presumably due to reduced reactivity of the first amination product. It appears that while the bidentate ligands successfully suppress the undesired β-hydride elimination, the catalyst complex is not active enough for the cyclization step (the second amination).
(41) The oxidation potential of nitrogen-substituted thiophenes has been shown to be very sensitive to changes in nitrogen substitution. See ref 36.
(42) Song, C.; Swager, T. M. *Macromolecules* **2005**, *38*, 4569–4576.